Thermo-mechanical behaviour of a thermo-active precast pile

Cristina de Santiago[1 *], Fernando Pardo de Santayana[1], María de Groot[1], Borja Badenes[2], Teresa Magraner[2], Javier F. Urchueguía[2], José Luis Arcos[3], Francisco Martín[3]

[1] Laboratorio de Geotecnia (CEDEX) C/ Alfonso XII, 3 y 5. 28014, Madrid (Spain)

[2] ITACA Institute - Universitat Politècnica de València. Camino de Vera s/n. 46022 Valencia (Spain)

[3] Grupo Rodio Kronsa. C/ Velazquez, 50-5ª 28001 Madrid (Spain)

* Cristina.desantiago@cedex.es

Keywords: geothermal energy, thermo-active pile, thermo-mechanical behaviour, thermal loads.

ABSTRACT

Please A new research and development project has been launched in Spain to undertake some studies on the geothermal use of pile foundations (PITERM PROJECT). The experiment, consists of a specifically designed, constructed and fully monitored geothermal precast pile driven at Polytechnic University of Valencia. The pile is under two types of loads: mechanical and thermal. The mechanical load was applied by means of a mechanical frame anchored to the ground, as element of reaction, and three anchors used to induce an active compressive force. The thermal load was provided by a thermal installation, with a data logger to record the outflow and return temperatures. The testing set is fully instrumented in order to register the thermo-mechanical behaviour of the system in terms of thermally induced movements, thermal axial strain profiles and shaft resistance mobilized as a result of cooling and heating. The results obtained permitted the quantification of three significant effects brought about by the temperature increase: pile uplift, additional load generated in the pile by constrain of the thermal stains, and mobilization of side friction due to the relative displacement of the pile with respect to the ground. The pile strain is of the thermo-elastic type and is strongly affected by the type of surrounding soil.

1. INTRODUCTION

Energy piles (thermo-active piles or geothermal piles) are foundations with double usefulness: to support the loads of the building and to serve as a heat exchanger with the ground. The geothermal use of pile foundations is a useful, efficient and cost effective method of installing ground heat exchangers for cooling and heating buildings. The key factor in the sustainability of thermo-active foundations systems is utilizing geo-structures that are already needed for structural purposes. This way, coupling piles with ground source heat pumps only requires a low extra over cost for geothermal installation, and it supposes a minimal impact on the piling program. They constitute a growing energy technology that improve the energy efficiency of heating and cooling systems in building and have been widely developed and researched in recent years [1, 2, 3, 4, 5, 6, 7] but it is still necessary to understand how the thermal and mechanical loads affect the mechanical behaviour of the pile. On the other hand, as this is a relatively new technology, robust standards and guidelines have not yet been developed for the design of these systems.

Although it is widely accepted that energy piles foundations are an efficient solution for long-term carbon emission reduction and sustainable construction, they have received only partial acceptance, because of concerns regarding the impact of cyclic thermal changes on their serviceability. In this sense, specific research is still needed to better understand how the thermal loads affect the pile behaviour: changes in vertical strains, stresses and axial loads along the pile, changes in shear stresses between pile shaft and soil, movements at head and toe of pile, changes in soil strength parameters, influence of ground lithological profile and water table position, effects of constrictions at head and toe of pile, possible associated phenomena regarding soil consolidation or negative skin friction, etc.

A research and development project in energy piles was performed in Spain from 2011 to 2015 (PITERM PROJECT). The purpose of this experiment was to improve the knowledge and understanding the effects of cooling and heating on precast piles subjected to mechanical loads in terms of mechanical, geotechnical and thermal actions.

2. PILE DESIGN AND CONSTRUCTION

A geothermal precast concrete pile was specifically designed and constructed at the Rodio-Kronsa factory (Fig. 1).



Figure 1: Precast pile at the factory Rodio-Kronsa

This test pile, made of reinforced concrete with characteristic resistance (f_{ck}) of 50 N/mm2 and a Young modulus of 31314.27 N/mm2 ($E=8500\cdot(f_{ck})1/3$), with a square cross section of 35 cm side and a total length of 17.4 m, was made of two pieces 8.70 m long each, connected by a joint. To activate it thermally, two polyethylene tubes were installed vertically within a steel pipe, 11.3 cm nominal diameter, located in the centre of the pile with a double U-shaped configuration to permit the passage of the heat carrying fluid.

Ground conditions of the testing site in Valencia were taken into account to the foundation design: A superficial fill layer of sandy gravel (1m thick); a second layer of stiff clay (1 m thick); a 6 m thick layer of soft and black organic clays; a 3 m thick layer of loose sands; and below depth 11 m, layers of sandy gravels extended up to a depth of at least 27 m, interlayered with some stiff clays levels. The ground water table is located at a depth of 2.0 m. Under these lithological conditions, the pile should work transferring loads to the soil levels located at more than 11 m of depth.

The ultimate compressive resistance of the pile, calculated from ground test results by the method established in the Spanish Building Code [8], was 2568,2 kN. Subsequently, a service compression load of 981 kN was decided at the pile head.

The pile was fully instrumented before being cast in the factory. The aim of the instrumentation was to monitor the distributions of temperature and axial strain with depth, as well as the supply and return temperatures of the heat exchanger fluid. Pairs of vibrating wire concrete-embedment strain gauges (VWSG) were oriented longitudinally and attached to the lateral reinforcing bars at seven different depths along the pile, then cast in concrete during construction (Fig. 2). Each VWSG contained a thermistor to monitor temperature in the concrete at each sensor location.



Figure 2: VWSG attached to the reinforcement bar

With the aim of comparing with the conventional instrumentation, Optical Fibre Sensors (OFS) were installed to measure temperature and vertical strain each 2 m along the length of the pile. Schematics of the foundation, the embedded sensors and the geological profile is shown in Fig. 3 and Fig. 4.

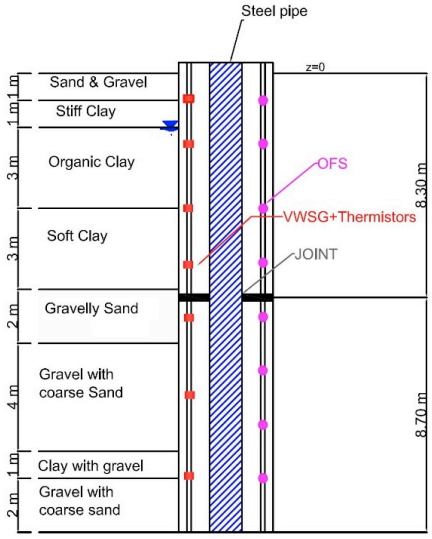


Figure 3: Soil profile and instrumentation

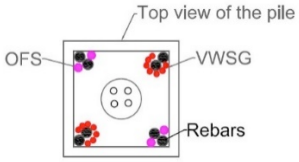


Figure 4; Top view of the pile

4. EXPERIMENTAL SET UP

The pile was driven into the soil the 27th of June, 2012 in Valencia. Driving tests were carried out to assess the ultimate vertical compressive resistance, resulting in a base resistance of 1800 kN and a shaft resistance of 711 kN. The pile was then subjected first to static load tests, and secondly to thermal tests by maintaining the mechanical service load of 981 kN. Therefore, two types of load application systems were needed: mechanical and thermal.

The mechanical load was applied by means of a metallic frame, as element of reaction, fixed to the ground by means of three 25 m long anchors, with an inclination of 5º. The compressive force was applied to the pile head by a hydraulic jack. A calibrated load cell measured the real load throughout the test (Fig. 5).

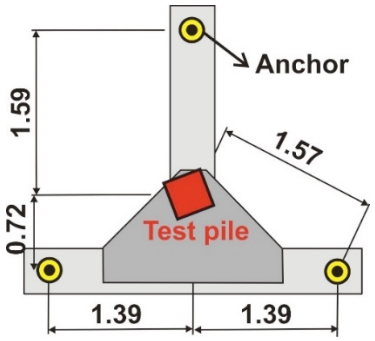


Figure 5: Scheme of the mechanical loading system

The thermal load was provided by a thermal installation (Fig. 6), formed by a reversible heat pump, a tank, a three-way valve for regulating the temperature of the injected water, a flowmeter and temperature probes with a data logger to record the inflow and outflow temperatures during the test.

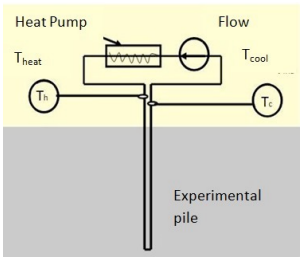
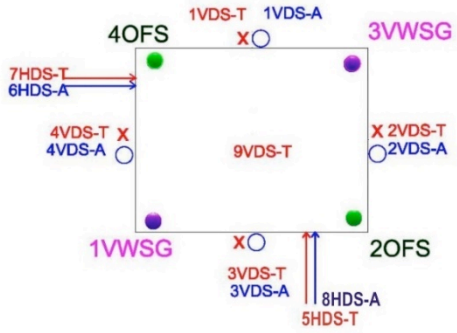


Figure 6: Thermal loading system

Once the pile was driven into the soil and thermally activated, the steel pipe located in the centre of the pile was filled with high thermal conductivity mortar (λ = 2.1 W/mK) made up of quartz sand and sulphate resistant cement. The characteristic resistance of this grout material is almost equal to that of the concrete used in the pile.

The initial temperatures recorded by all the sensors prior to start the initial load test were between 17ºC and 21ºC. Below 10.40 m depth the ground temperature remains constant at 19ºC.

Finally, additional sensors were installed outside the pile, in strategic points of the loading frame and anchors, in order to monitor the pile behaviour during the thermal and mechanical loads (Fig. 7 and Table 1).



VDS-T: Vertical displacement transducer: LVDT
VDS-A: Vertical displacement analog dial gauge
HDS-T: Horizontal displacement transducer: LVDT
HDS-A: Horizontal displacement analog dial gauge
OFS: Optical fibre sensors
VWSG: Vibrating wire strain gages

Figure 7: External sensors on the pile head

Table 1: Total monitoring during the study

Test element	Monitoring
Test pile (external)	4 analog dial gauges for vertical pile head displacements 4 electronic transducers (LVDT) for vertical pile head displacements 2 analog dial gauges for horizontal pile head displacements 2 electronic transducers (LVDT) for horizontal pile head displacements 1 LVDT to loading frame Load cell
Test pile (internal)	VWSG at seven levels in rebars diametrically opposed over 17 m length of pile OFS cables, 2 loops for strain and temperature measurement at the same time placed each loop diametrically opposed
Anchors	VWSG in each anchor to measure strain and temperature

The Fiber Optics Sensors, based on fiber Bragg grating (FBG) technology, are intended exclusively for embedding in concrete structures. Although the technical sheet of these sensors offer nominal wavelength for 22ºC (λ_{22}) and a temperature sensitivity constant value (St) of 23.8 pm/ºC, a lab-calibration was performed prior to their installation within the energy pile. In this manner, all the individual real λ_{22} and St values were determined to allow the later conversion of the raw signals into temperature and strain values.

As for the VWSG sensors, the ideal methodology to measure the global thermal correction factor would have involved measuring the axial heave of the energy pile during heating before applying the mechanical load of 1000 kN and comparing this with the measured thermal axial strains using a soil-structure interaction analysis such as that of Knellwolf et al. [9]. In the absence of this type of test, the calibration factor given by the factory (12.2 μm/m·ºC) was used in calculations.

5. FIELD ASESSMENT OF THERMAL PERFORMANCE

Energy pile (EP) design needs to integrate geotechnical, structural and thermal considerations. The geothermal heat exchange capacity of an energy pile is a key design parameter to dimension the

geothermal loops and the heat pump system. Thermal characteristics of the ground as well as the heating and cooling loads from the structure need to be considered for the number of EPs that will be utilized as heat exchangers. Therefore, the thermal properties of the site need to be evaluated in addition to the geotechnical characterization for foundation design. In this project, the first test performed to evaluate the thermal behaviour of the experimental EP has been a thermal response test (TRT).

TRT is a widely used field method for estimating soil thermal conductivity and the thermal resistance of traditional borehole heat exchangers (BHE). However, there is a lack of scientifically supported guidelines for analysing TRT data from energy piles [10]. Recently, the Ground Source Heat Pump Association (GSHPA) published a manual on the design and construction of energy piles [11], including TRT guidelines for EP. Testing methods for BHE systems assume a high length to diameter ratio so that the shape of the borehole approaches a line source. The diameter of an energy pile is significantly larger and the depth is typically much less. The difference in geometry means that the testing practices of BHEs do not necessarily apply to EPs, for this reason, the GSHPA association has made some recommendations in regards to conducting TRTs for EP systems:

1. When the potential use of EP systems is identified early in the design process a BHE can be constructed with a single loop and tested to find the local thermal properties.
2. If the designed piles are no larger than 30cm in diameter, a TRT can be carried out using the recommendations made for a BHE system.
3. If the EP system design consists of piles larger than 30 cm in diameter, the TRT should be extended to ensure that the thermal resistance of the pile is overcome. Furthermore, more sophisticated interpretation techniques can be applied.
4. Once the EP is fully instrumented with strain gauges and temperature gauges, it is possible to conduct a complete stress-strain analysis as well as a thermal analysis in order to better understand the structural and thermal behaviour of the pile under the superimposed action of coupled mechanical and thermal loads.

Since the experimental energy pile is square section 0.35 m side, and bearing in mind the recommendations of GSHPA, the field assessment of thermal performance in this project consists of two different tests: firstly, two bespoke TRT of longer duration (5 + 6 days) were performed to ensure that the thermal resistance of the pile is overcome. Then, as the EP is fully instrumented with VWSG extensometers, thermistors and Fiber Optics Sensors, a complete stress-strain analysis was undertaken in order to better understand the structural and thermal behaviour of the pile under the superimposed action of coupled mechanical and thermal loads.

6. THERMAL LOADS GENERATING FACILITY

The main objective of the facility is to produce the thermal heat injection and to monitor the associated variables that allow to perform the thermal response test analysis.

In order to produce thermal loads, the appliance uses a reversible heat pump (cooling) or a thermal resistance (heating) and a hydraulic circuit. Several measurement elements and electronic circuits are necessary for the required data-logging and measurement control. The facility is shown in figure 8 schematically.

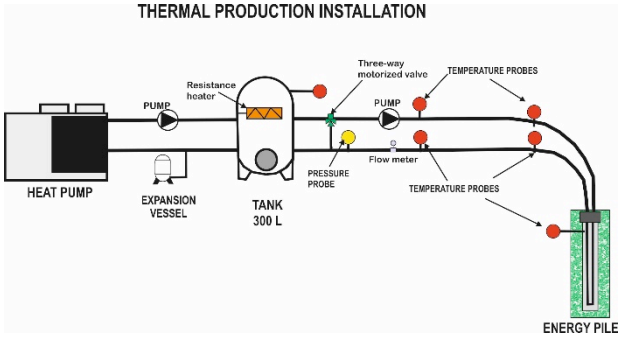


Figure 8: Thermal loads generating facility

Throughout the test, water is circulated into the thermo-active pile and heat is exchanged with the surrounding soil through the pipes located inside, in a thermo-hydraulic configuration alike any conventional BHE.

The system contains two cycles of water flow:

1. The primary cycle, which contains the heat exchanger pipes, installed in the pile, the primary circulation pump, a three-way valve for regulating the temperature of the injected water, a flow meter and various temperatures probes.

2. The secondary cycle, which contains the heat pump, a storage tank equipped with a thermal resistance, an expansion vessel and the secondary circulation pump.

The primary cycle is responsible for maintaining a constant power supply to the experimental pile, maintaining a constant temperature difference between inlet and outlet of the pipe installed in the pile in order to activate it thermally. For this purpose, the secondary circuit supplied water heated or cooled by the thermal resistance or the heat pump. The temperatures of the heat exchange fluid entering and exiting the pile during heat pump operation were monitored using a pipe-plug thermocouples installed in the inlet and outlet ports of the manifold. The fluid will be able to extract or inject heat into the ground depending on the relationship between the

temperatures of the heat carrier fluid and the ground around the pile at each moment throughout the test.

Summarizing the main characteristics of the facility:

- Cold generation (heat pump) and heat generation (electric resistance).
- Regulation of the injected power by means of pulse width modulation.
- Monitoring of the flow, inlet and outlet temperature and pressure.
- Remote control of the process.
- Data logging.

3. THERMO-MECHANICAL BEHAVIOUR OF THE PILE

In addition to the heat exchange design for energy foundations, geotechnical design is also needed. Geotechnical design requires consideration of the complex interaction between temperature change and induced stresses and strains in the foundation, which may affect building performance. Specifically, contraction or expansion of the foundation during cooling or heating may lead to mechanical distress movements of the structural foundation elements or the building itself, as well as changes in pile shaft shear stresses and base loads and, therefore, in the factors of safety for bearing resistance of the foundation. An important aspect of this study was to evaluate thermally induced axial strains and stresses in the energy foundations caused by temperature changes.

The parameters measured and registered by VWSG and FOS were quite similar, both in relative values and in trends with depth and temperature.

The first step to define the thermal axial strain is to isolate the effect of the mechanical loading. To achieve this, an initial measurement was performed under a mechanical load of 1000 kN, without any temperature action upon the pile. From this initial measurement onwards, the value of mechanical component of the strain after this point is considered constant, assuming that there is negligible variation in the mechanical load applied to the pile head over time. Accordingly, the measured strain values ε_m were zeroed by subtracting the mechanical axial strain. Next, the zeroed strain values were corrected to account for thermal effects on the gauge, by a correction factor ($\alpha \cdot \Delta T$), where α is the coefficient of linear thermal expansion of the steel wire in the gauges (-11με/ºC) and ΔT is the temperature change of the pile.

The "test C" is meant to show the thermo-mechanical behaviour of the pile under a constant and stable mechanical load of 1000 kN and a wide range of thermal loads, simulating its use within a geothermal installation working on summer mode (cooling the building and heating the foundation). This test was performed between 26th of June and 10th of July of 2013, following the schematic and stages shown in the Fig. 11. These three stages correspond to different heat injection rates by applying different power values (Table 2).

Table 2: Stages of the test C

	Stages		
	1	**2**	**3**
Initial date	26/6/2013	01/7/2013	05/7/2013
Initial hour	11:09	12:33	12:03
Final date	01/7/2013	05/7/2013	10/7/2013
Final hour	11:06	11:12	13:30
Fluid	Tap water		
ΔTºC	1ºC	3ºC	1.5ºC
Applied power (W)	700	2100	1050
Heat injection rate (W/m)	40	120	60

In order to define profiles of thermal axial strain representative of the pile performance, some specific moments in time were identified. All of them were chosen at the end of each thermal stage, after a time enough to reach thermal equilibrium in the system (Table 3 and Fig.9).

Table 3. Strategic moments identified during test C

Moment	***Date and hour***	***Observations***
C0	26/06/2013 10:57	Prior to test C
Ca	01/07/2013 12:27	After thermal equilibrium at stage 1
Cb	05/07/2013 12:27	After thermal equilibrium at stage 2
Cc	10/07/2013 14:30	After thermal equilibrium at stage 3
Cd	11/07/2013 11:54	End of test C
Ce	30/07/2013 10:07	19 days after end of test C

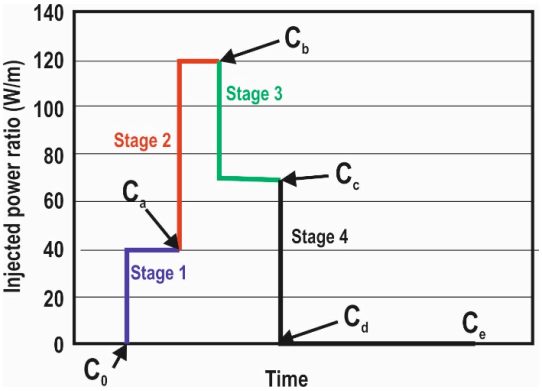


Figure 9: Schematic of the test C and identification of strategic moments: C0, Ca, Cb, Cc, Cd and Ce.

Throughout this test C, strains and temperatures, power and flow were registered, to be able to analyse any possible out of phase results regarding the thermal and the geotechnical behaviour of the pile.

3.1 Temperatures

Firstly, all the profiles obtained during the test show a temperature decreasing with depth. Near the surface the pile temperature is affected by both the injected thermal power and the atmospheric temperature variations. This phenomenon, well explained by McCartney & Murphy [11] and Bourne-Webb [5], results less important with the depth, were the pile temperature is much less affected by atmospheric temperature changes.

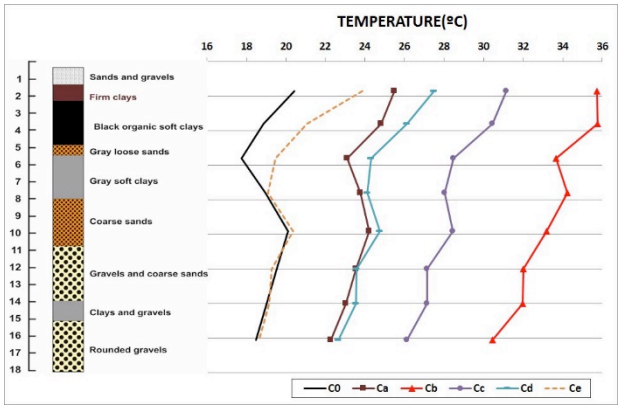


Figure 10: Temperature profile evolution during test C

Prior to starting the test C (C0), the ground temperature is more or less homogeneous around 19-20ºC. Once the test begins, the effect of heat injection in the temperature profile of the pile is clear: in Cb (after 120 W/m heat injection rate equilibrium is achieved) the temperature is 35-36ºC in the upper meters and 30-31ºC in the lower zone. In terms of temperature changes, comparing these values to the moment C0, the first meters of pile show a temperature increment of 17ºC, while 12ºC change is registered in the lower part of the pile. In Ca (after 40 W/m heat injection rate thermal equilibrium is achieved) the temperature profile is close to the one corresponding to Cd, after finishing the test. This verifies the fact that the pile needs some time delay to dissipate the high temperatures generated during heat injection. In Ce, after 19 days of thermal stabilization, the temperature profile comes back to the initial state (C0) in the deeper part of the pile. The 6 most superficial meters the Ce profile shows more temperature values than the C0 profile. This is due to the different climatological conditions and ambient temperature. While in C0 (26th of June) the ambient temperature was 22.9ºC, in Ce (30th of July) it was 29.8ºC.

Fig. 11 shows the thermal evolution of the pile in terms of temperature change with respect to C0. The close shape of the response at different depths along the pile shows a strong dependence of the thermal temperature changes on the heat injection rate at the different stages of the test.

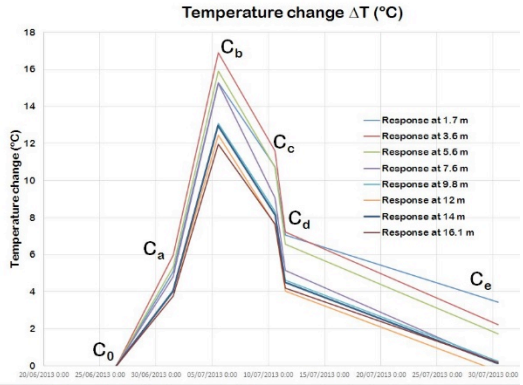


Figure 11: Temperature change detected at different depths throughout the test stages

Pile head movements

The sensors installed at the pile head allowed to measure in real time the vertical and horizontal movements generated due to thermal changes during the test C (Figs. 14 and 15).

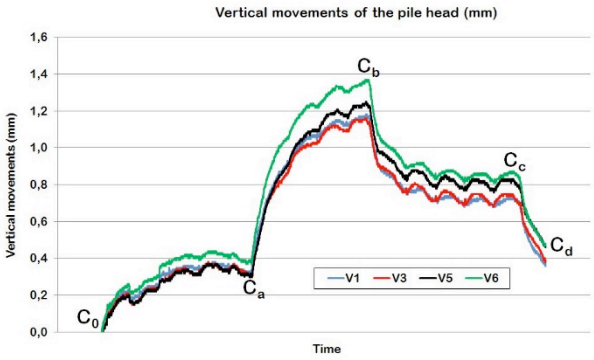


Figure 12: Vertical movements of the pile head during test C

The maximum vertical movements measured at the pile head were 0.4 mm in Ca (40 W/m injected), 1.4 mm in Cb (120 W/m injected), and 0.8 mm in Cc (70 W/m injected). After this moment, all the sensors showed a trend to diminish towards zero as the pile thermally recovered. Furthermore, a clear cyclic oscillation due to thermal daily variations can be detected. The pile head did not return to its original elevation upon cooling (Cd), but maintained an upward displacement of approximately 0.4 mm.

The horizontal movements of the pile head (Fig. 13) do not show the same clear correlation to the sequence of different stages throughout test C as vertical movements do.

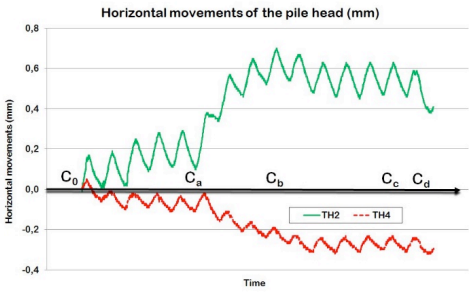


Fig.13. Horizontal movements of the pile head during test C

TH2 sensor measured a movement towards a maximum +0.6 mm, while TH4 sensor moved towards -0.3 mm. These two components give a resultant movement of 0.65 mm towards South-Southeast. The daily oscillation is very evident.

3.2 Strains

When a pile under working load is heated or cooled, a complex behaviour is imposed upon the pile that varies with ground conditions and different degrees of end restraints. The heating of a pile induce expansion while cooling induces contraction leading to pile vertical strains, displacements of the pile head and changes in shaft friction and base stresses. The total strain due to mechanical and thermal loads (ε_T) is:

$$\varepsilon_T = \varepsilon_m + \varepsilon_{th}$$

Where ε_m is the strain due to a mechanical load and ε_{th} is the strain due to the thermal loads.

Thermal free strains

Thermal deformations (Fig. 16) may occur in energy foundations due to thermo-elastic expansion, in which thermal strain ε_{th} occurs during a change in temperature proportionally to this change, by means of a coefficient of thermal expansion. Considering a theoretical unrestrained pile, the change in temperature induces a uniform free strain [12]:

$$\varepsilon_{th,f} = \alpha \cdot \Delta T$$

Where α is the coefficient of thermal expansion of the pile (11 μm/m·ºC).

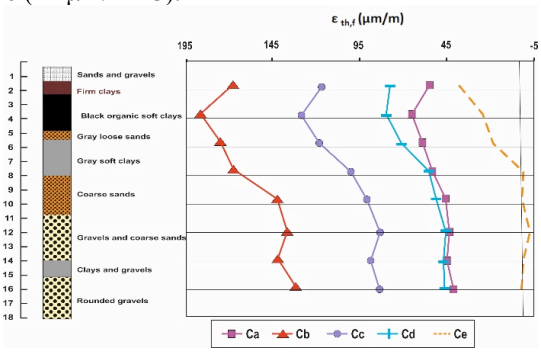


Figure 14: Theoretical thermal unrestrained strains in a completely free of movements pile ($\varepsilon_{th,f}$)

Observed strains

Actually, the energy pile is far from unrestrained. The surrounding soil provides a confining effect on the pile, constraining the possible deformations. For this reason, depending on soil-structure interaction conditions, the real expansion or contraction observed and measured (ε_{obs}) by the VWSG extensometers within the energy pile due to the applied thermal loads results much lower than the theoretical free thermal unrestrained strains calculated previously from the temperature change measured in the pile. The profiles of observed axial strain induced by the thermal loads corresponding to the specific moments defined above are shown in Fig. 15. In these figures, negative strains indicate compression in the pile, while positive strains indicate expansion.

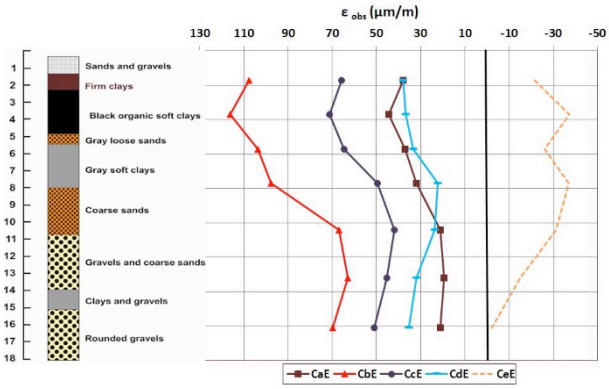


Figure 15: Observed deformation, measured by the VWSG extensometers

Regardless of the shapes of the mechanical strain profiles, it is clear that the heating operation led to a shift in the observed strain profiles to the left, towards positive values (expansion). Cooling after the test leads to a recovering and shift of the profile to the right, towards negative values (compression).

All the curves show positive values, corresponding to tensile strains, with the exception of the Ce profile, corresponding to 19 days after finishing the test C, where a 38 μm/m maximum compression strain was registered. The maximum tensile deformation is measured in Cb, when the heat injection is maximum, as well as the temperature measured in the pile. In Cd, just after the cessation of heat application, a 40 μm/m tensile strain was measured. The shape of the strain profiles depends not only on the temperature changes, but on the resistance the ground around the pile offers to its deformation. With this view, higher deformation values are measured in the upper part of the pile, at all the heat injection curves, while the deeper part of the pile tends to show lower strain values. This can be explained partially by the different geological strata surrounding the pile. The upper meters of ground are composed of soft clayey materials, which offer less resistance to the dilation of the pile than the gravels existing in the lower meters of the pile.

From the strain data obtained at different depths, the whole elongation of the pile can be calculated. At

moment Cb, under the action of a heat injection rate of 120W/m, the pile exhibits a maximum elongation of +1.6 mm. Meanwhile, the maximum pile head vertical movement measured by the LVDT's is +1.23 mm. By comparing these two values (Fig. 16), a settlement of the pile toe of 0.37 mm is deduced.

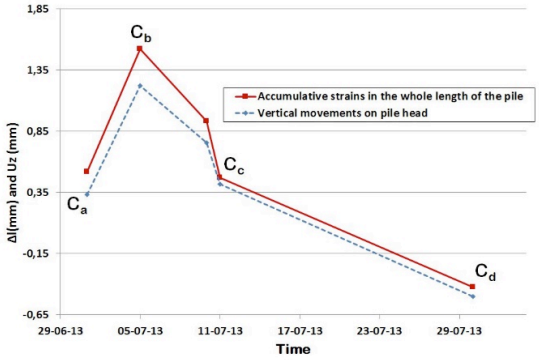


Figure 16. Comparison between the accumulative strains along the pile and the vertical movements measured on pile head.

Thermal constrained strains

Since part of the pile deformation is constrained by the surrounding soil, a blocked, non-produced, strain has to be considered:

$$\varepsilon_{th,c} = \varepsilon_{th,f} - \varepsilon_{obs}$$

The thermal constrained axial strains profiles corresponding to the different moments of the test C, measured by the FOS, are shown as a function of temperature in Fig. 19.

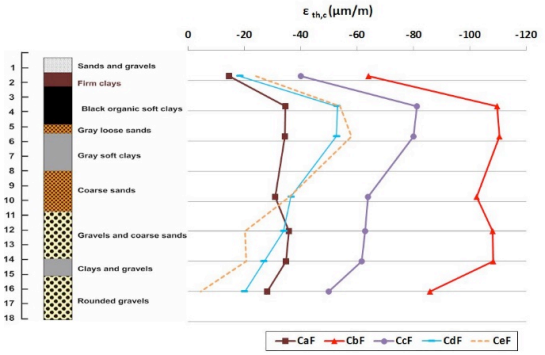


Figure 17: Thermal constrained strains during test C

It is worthwhile to remark that the thermal constrained strain values in the first meter trends to zero in all the curves, as there are no restrains to dilatation at the pile head, where the mechanical load stays constant.

Stresses

Thermal stresses

The average thermal axial stresses induced in the foundation by the temperature changes (kN) can be calculated from the measured thermal axial strains at the location of each gauge as follows:

$$\sigma_{th} = E \cdot \varepsilon_{th,c}$$

Where $\varepsilon_{th,c}$ is the average thermal axial strain (μm/m) and E is the Young's modulus of the pile (313142.7 MN/m^2).

The calculated thermal (σ_{th}) and total ($\sigma_{th+mec} = \sigma_{mec} + \sigma_{th}$) axial stress profiles are shown in Fig. 18 and 19. In these figures, negative stresses indicate compression while positive values indicate extension.

Comparison of this figure with the evolution of strains allows seeing that the locations of the smallest strain in the energy pile (where the pile is surrounded by stiff sands and gravels) correspond to the locations of the maximum thermal axial stress, possibly due to the resistance to thermal axial expansion by mobilization of shaft shear stresses. In other words, compressive (negative) thermal axial stresses occur during heating of the pile (cooling of the building) when the axial expansion of the foundation is restrained by ground at the pile/soil interface and at the pile base.

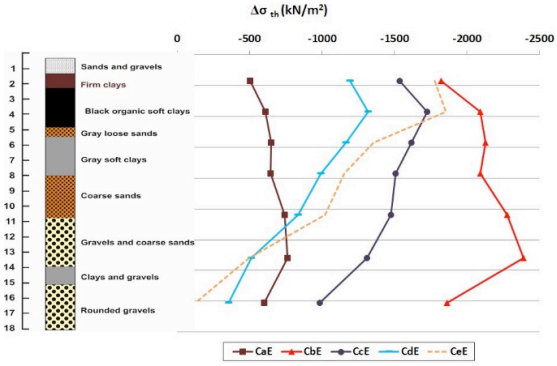


Figure 18: Thermal axial stress due to heating and cooling during test C

Total stresses

The thermal axial stress profiles observed during heating and cooling of the pile were superimposed upon the stress profile due to mechanical loading (1000 kN) to define the total thermo-mechanical axial stresses (Fig. 19).

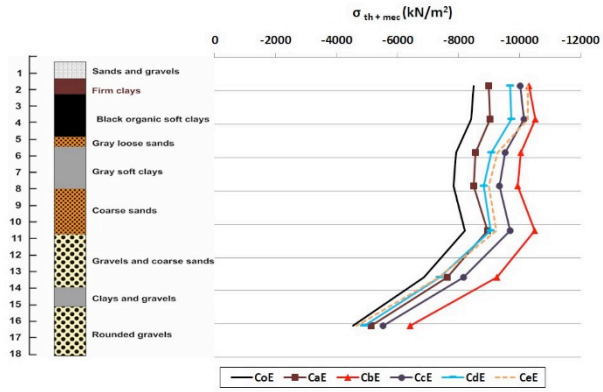


Figure 19: Total axial stress evolution throughout the test C

Two main different zones can be distinguished in the pile: an upper part, between 2m and 10 m of depth, where the surrounding ground consists of soft soils (soft clays, organic clays and loose sands), that shows

an almost vertical profile; a lower part of the pile, from about depth -10m, showing a diminishing stress towards the pile toe, as a consequence of the presence of stiff gravels and sands with a higher frictional resistance. Comparing Figs. 20 and 21, it can be seen that the thermal axial stresses are clearly lower than the mechanical axial stresses; nevertheless, they are not at all insignificant (about 2500 kN/m2 of maximum thermal stress, relatively to 8163 kN/m2 of maximum mechanical stress).

3.3 Loads

The thermal and total stresses profiles can be converted into thermal and total load profiles respectively (Fig. 22 and 23), by simply using the following equation:

$$N = \sigma \cdot S$$

Where N is the axial load (kN), σ is the average stress in the corresponding section (kN/m^2) and S is the area of the pile section (S = 0.35·0.35 = 0.12 m^2)

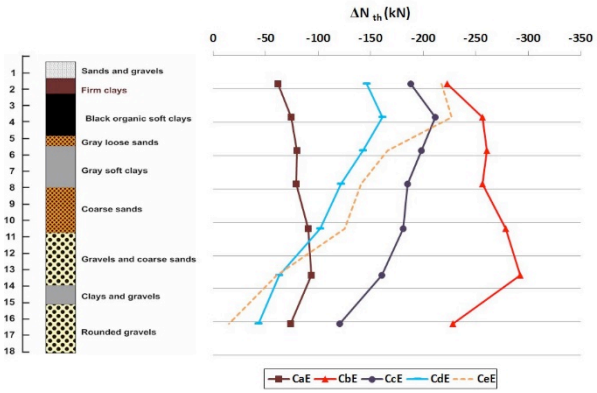


Figure 20: Thermal axial load profiles during test C

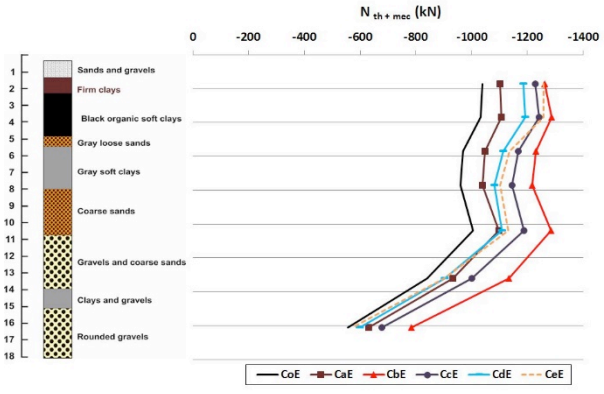


Figure 21: Total axial load profiles during test C

Pile/soil interface shear stress

It is worthwhile to remark how the thermal and total shear stresses originated along the pile shaft (Fig. 22 and 23) are related to the heat injection in the pile.

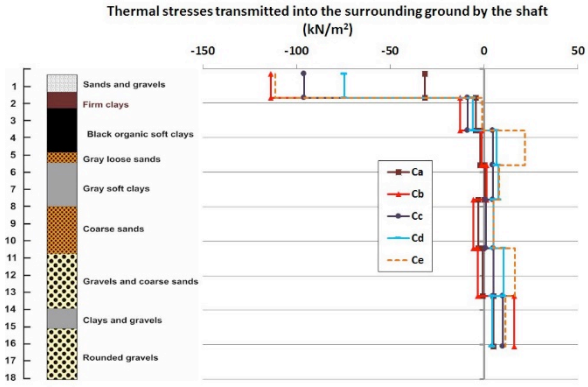


Figure 22: Thermal shear stresses along pile shaft during test C (kN/m2)

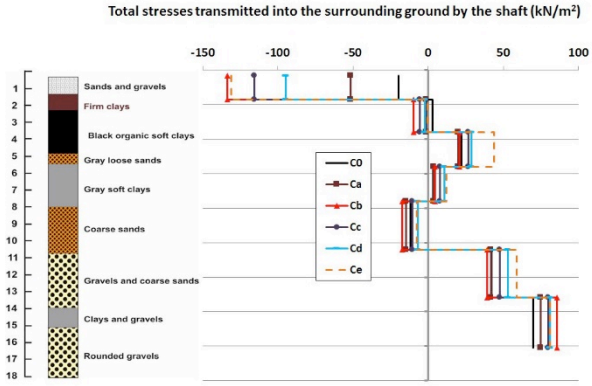


Figure 25: Total shear stresses along pile shaft during test C (kN/m2)

Heating the pile results in dilatation deformations. As a result of the tendency of the surrounding soil to constrain the pile dilation, the mobilized shaft friction during heating shows an opposite response at the upper part, where the friction is negative (the soil is exerting a downwards force on the pile shaft), and the lower part of the pile, where the friction is positive (the soil is exerting an upwards load on the pile shaft). The opposition to pile dilation is not uniformly distributed along the pile depth, but depends on the ground profile, specifically on the existence of soft or stiff soil levels. Only those layers of stiff or very frictional materials will be able to oppose the pile dilation or contraction. On the other hand, at the depths where the pile is surrounded by soft soils, the opposition to thermal dilation or contraction of the pile will be negligible. In this experimental case, it appears that the opposition to pile dilation is concentrated at both ends of the pile, at the upper 2 metres, where the soil consists in artificial fills and stiff clays, and at the toe area, where the soil is composed of coarse sands and gravels. This evidences the importance of the stratigraphic column in the thermo-mechanical behaviour of the system.

This trend to dilation inverts during moments Cc and Cd, when the pile cools down with respect to Cb. During this process, the soil tends also to show a stronger opposition to pile contraction at both ends.

In summary, pile/soil interface shear stresses generated due to heat injection into the pile during the test C, are coherent with the theoretical model and with the explanations published by Bourne-Webb et al. (5), with some specific peculiarities derived from the local geological profile, offering two main zones of stiff lithologies that can constrain the potential pile deformation: the upper 2 metres and the toe zone. During the cooling part of the test C (Cc, Cd moments) the thermal inertia of the soils surrounding the pile are also determinant in the evolution of the profiles.

4. CONCLUSIONS

This work presents the results from a thermo-mechanical evaluation of a full-scale precast energy pile, under a constant and stable mechanical load of 1000 kN and a wide range of thermal loads, simulating its use within a geothermal installation working on summer mode (cooling the building and heating the foundation).

Data collected from both types of sensors allowed to assess the thermo-mechanical behaviour of the pile in terms of axial strains, stresses and loads, as well as pile/soil interface shear stress values. Thermal and total axial strains measured are consistent with a pile predominantly working at its toe. It is important to notice that the thermal loads applied during the test C, described in this paper, are probably higher than those that would be needed in a real case of geothermal exploration of a normal office or residential building founded on piles like the one used in this study. Nevertheless, the thermal impacts on the mechanical response of the pile would not likely lead to significant structural problems. Anyhow, an analysis of the effects of both the mechanical loads and the thermal loads is considered necessary for a proper design of thermo-active piles.

Further research is still needed to improve the understanding of the thermo-mechanical behaviour of geothermal piles and to formalize design guidelines and safety factors for assuring the ultimate and serviceability limit states of the energy foundations.

REFERENCES

1 L. Laloui, M. Moreni & L. Vulliet, *Can. Geotech.* J. **40**, 388-402 (2003).
2 L. Laloui, M. Nuth & L. Vulliet, *International Journal for Numerical & Analytical Methods in Geomechanics,* **30, No 8**, 401, (2006).
3 H. Brandl, *Geotechnique,* **56, No 2**, 81, (2006).
4 A. Amis, P. Bourne-Webb, B. Amatya, K. Soga, & C. Davidson, *3rd Ann. and 11th Int. DFI Conf., New York*, 10 pp (2008).
5 P. Bourne-Webb, B. Amatya, K. Soga, A. Amis, C. Davidson & P. Payne, *Géotechnique,* **59**, 237 (2009).
6 L. Laloui & A. di Donna, *Civil Engineering*, **164**, 184, (2011).
7 B.L. Amatya, K. Soga, P. Bourne-Webb, T. Amis & L. Laloui, *Géotechnique,* **62**, 1, (2012).
8 Código Técnico de la Edificación – Documento Básico de Seguridad Estructural (DB-SE C, 2006)
9 C. Knellwolf, H. Peron & L. Laloui, *Journal of Geotechnical and Geoenvironmental Engineering,* **137, No 10**, 890 (2011)
10 F. Loveridge, *Ground Source Seminar, Homerton College, Cambridge University,* (2011)
11 H. Park, S.R. Lee, S. Yoon & J.C. Choi, *Applied Energy,* **103**, 12, (2013).
12 J.S. McCartney & K. Murphy, *DFI Journal*, **6 No 2**, 26, 2012

Acknowledgements

We thank the Spanish Ministry of Economy and Competitiveness for its financial support, through the program INNPACTO 2011, for the design, installation and instrumentation of the geothermal pile in Valencia.

